Enhancement of Film Condensation Rate on Vertical Tubes By Longitudinal Fins

DAVID G. THOMAS

Oak Ridge National Laboratory, Oak Ridge, Tennessee

Longitudinal rectangular fins loosely clamped to vertical tubes markedly increase the film condensation heat transfer coefficient. At a heat flux of 2 × 10^4 B.t.u./hr.sq.ft., twelve 1/8 × 0.013 fins clamped to a ½ in. O.D. vertical tube 42½ in. long (thus doubling the surface area of the tube) gave a condensation coefficient of 15,000 ± 15% B.t.u./hr.sq.ft. °F. compared with 1,620 B.t.u./hr.sq.ft. °F. for the same tube without fins, a ratio of h/h_o of 9.2. The enhancement of the film condensation coefficient decreases as the heat flux increases and as the number of fins decreases.

A model based on the effect of fin shape on film and rivulet hydrodynamics explains the observed behavior.

Film condensation characteristics of vertical tubes with grooved surfaces [that is, fluted tubes (*1* to *4*), Figure 1] are markedly better than those of smooth tubes. The increase in the heat transfer coefficient is due to the extremely thin liquid film remaining on the crest of the flutes as the bulk of the condensate is drawn to the troughs where it flows rapidly down the tube. The flow of condensate from the crest to the grooves is induced by surface tension forces which are developed whenever the liquid-vapor interface is not plane. The magnitude of the surface pressure difference across the interface between vapor and liquid is given by Laplace's formula (*5*)

$$p_1 - p_2 = \sigma\,(1/R_1 + 1/R_2) \qquad (1)$$

with greater pressure in the medium whose surface is convex. The shape of the fluted tube surface was believed (*1, 2*) to be a critical factor in developing the surface tension force which draws the condensate from the crest to the troughs of the flutes. Therefore, considerable care was necessary in the design and fabrication of the fluted surface. The procedure (*1, 4*) for calculating the surface profile was to combine Nusselt's equation for flow in a thin film with (*6*) with continuity equation and the condensate growth equation for a small circumferential element of surface profile. Then by assuming the pressure gradient from crest to trough was given by Equation (1) and that the condensate film thickness was a constant over the profile of the fluted surface and initial values for the crest radius of curvature and the film thickness, the remainder of the surface profile was calculated by numerical integration. With these assumptions, the positive pressure at the crest of the flute was calculated (*1*) to be substantially larger than the negative pressure in the trough.

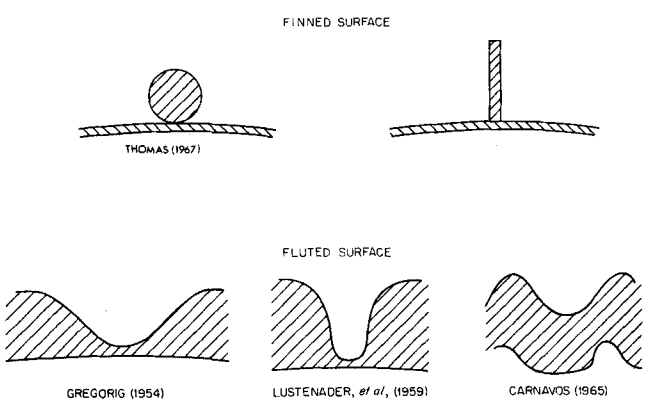

Fig. 1. Profile of surfaces for enhancing film condensation (not to scale).

The discovery (7) that small longitudinal wires loosely attached to vertical condenser tubes causes a pronounced increase in the rate of film condensation made it clear that a fluted contour of the solid surface was not necessarily a critical factor in inducing three dimensional motion of the condensate by surface tension effects. The object of this study was to extend the previous studies with round wires to shapes of rectangular cross section (that is, longitudinal fins) in order to develop a surface which was easier to manufacture and at the same time to maximize enhancement of the rate of heat transfer and minimize flooding effects.

SIMPLIFIED MODEL

Enhancement of film condensation by modification of the surface profile of the tube requires that all surfaces exposed to vapor be wetted by condensate. Then, when the initial steam condenses on the finned tube surface, a thin film covers both the tube and the fin. At the junction of the fin and the tube, the surface of the water film is curved. Because of surface tension, there is a difference in surface pressure [given by Equation (1)] between the fluid in the corner and the fluid on the tube surface which causes fluid to flow from the tube surface to the corner. The bulk of the condensate is rapidly carried down the tube as a small rivulet flowing along the fin, leaving only a very thin film on the remainder of the surface of the tube where very large condensation coefficients can occur.

In a previous paper, (7) a model was developed which described the dependence of film condensation enhancement by longitudinal wires on a number of wires and heat flux. The principal assumptions on which the model was based are:

1. Flow can be divided into a rivulet flowing along the wire and a thin film over the bulk of the tube.
2. Because the wires were not in good thermal contact with the tube, there was negligible heat transfer beneath the wires and the rivulets.
3. The pressure gradient which draws the fluid from

the surface to the rivulet in the fin corner is proportional to the right side of Equation (1). Then by combining a mass balance, dimensional analyses and knowledge of flow in thin films and rivulets, (6, 8) it was possible to develop an expression for the ratio of condensate film thickness without wires to film thickness with wires (and hence the enhancement of film condensation coefficient as a function of heat flux and number of wires) which contained only one empirical constant:

$$\frac{h}{h_o}=\left[\left(1-\frac{2.5Nd}{\pi D}\right)+\alpha\left(\frac{Nd}{\pi D}\right)^{5/2}\left(\frac{g_c\sigma L}{\Gamma\nu}\right)^{3/2}\right]^{11/3}\left(1-\frac{2.5Nd}{\pi D}\right) \quad (2)$$

with $\alpha = 1.7\ (\pm 0.3) \propto 10^{-6}$. The terms in the square bracket on the right give the ratio of condensate film thickness without fins to the condensate film thickness with fins and the term in the round bracket on the far right is a correction for the amount of tube over which heat transfer was negligible due to the wires and rivulet. Equation (2) fitted the data extremely well except at the highest heat flux where flooding might be important.

The numerical coefficient 2.5 in the terms on the right of Equation (2) was obtained assuming the radius of curvature of the water rivulet is a constant fraction of the wire diameter, independent of the heat flux. The empirical constant α contains average numerical coefficients from expressions for hydraulic diameter, laminar friction factor, and radius of curvature of the water rivulet as well as the unknown factor relating the surface tension to the pressure difference which draws the condensate from the tube surface to the wire. Because the wires were all cylindrical, (7) all these terms could be lumped into the one coefficient, α. (Note that, although the three dimensional flow equations can in principle be solved for free surface flows in which surface tension and temperature gradients are included, such solutions have not been obtained. The main obstacle is that the surface tension must be applied as a boundary condition to the free surface (5) and the shape of the free surface is the major unknown determined by the surface tension.)

In the following sections the model developed in the previous paper (7) will be extended to account for the effect of fin shape (rectangular or cylindrical) and condensation rate on rivulet dimension. Such an extension will permit estimates of flooding conditions as well as predicting heat transfer enhancement. A test of whether fin and rivulet geometry factors have been satisfactorily accounted for will be whether the coefficient relating surface tension and pressure drop is the same for both cylindrical and rectangular fins.

The additional assumption required to extend the model are that the shape of the surface of the rivulet is cylindrical, that substantially all of the condensate flow is in the rivulet and that the thickness of the film is small compared to the radius of curvature of the rivulet. Then by defining l as the distance between fins over which large heat transfer coefficients may be expected, we obtain

$$l=\frac{\pi D}{N}-d-2R \quad (3)$$

Equation (2) becomes

$$\frac{h}{h_o}=\left[\frac{lN}{\pi D}+\alpha_1^{3/2}\left(\frac{0.418}{\alpha_2}\right)\left(\frac{D_H{}^3P}{R^{3/2}}\right)\left(\frac{g_c\sigma L}{\Gamma\nu}\right)^{3/2}\left(\frac{N}{\pi D}\right)^{5/2}\right]^{1/3}\left(\frac{lN}{\pi D}\right) \quad (4)$$

using the same terminology as the previous paper (7).

An approximate expression for the radius of curvature of the rivulet at the end of the tube may be obtained by equating the condensate carried off per fin to the volumetric flow rate in the rivulet, noting that there are two rivulets per fin

$$\frac{\Gamma\pi D}{2\rho N}=V_A A_1 \quad (5)$$

For laminar flow in the rivulet, the friction factor is given by

$$f=\frac{\tau_w}{\frac{\rho_f V_A{}^2}{2g_c}}=\frac{\alpha_3}{\frac{D_H V_A}{\nu}} \quad (6)$$

In the absence of drag at the free surface, the wall shear stress must support the total body force on the rivulet; that is

$$\tau_w=\frac{g_L}{g_c}\rho_f\frac{D_H}{4} \quad (7)$$

Combining Equations (6) and (7) gives

$$V_A=\frac{g_L D_H{}^2}{\alpha_3\nu} \quad (8)$$

By definition

$$A_1=\frac{D_H P}{4} \quad (9)$$

From the geometry assumed for the rivulet along rectangular fins, $D_H = 0.43R$ and $P = 2R$; a value of $\alpha_2 = 12$ was estimated from studies of Fulford (8), and Gunn and Darling (9). Then after accounting for the growth of the rivulet along the fin and assuming that the thickness of condensate on the fin projection was 10% of the radius of curvature, the value for the average radius of curvature from Equations (5), (8), and (9) is

$$R=\alpha_4\left[\frac{\nu\Gamma D}{g_L\rho N}\right]^{1/4}=1.6\left[\frac{\nu\Gamma D}{g_L\rho N}\right]^{1/4} \quad (10)$$

Parameters for rectangular and cyindrical fin cross sections are summarized in Table 1; the cylindrical fin parameters were estimated with the same assumptions as those given above for rectangular fins. The final equations for heat transfer enhancement are obtained by combining Equations (3), (4), and (10) and the values in Table 1.

Table 1. Parameters for Cylindrical and Rectangular Fin Cross Section

	Rectangular fins	Cylindrical fins
D_H	0.430	0.214 R
P	2 R	1.53 R
α_3*	12	7
α_4	1.6	2.4
β†	8.2×10^{-3}	8.2×10^{-3}

* Estimated from References 8 and 9.
† Empirical value.

Rectangular fins

$$\frac{h}{h_o}=\left[1-\left(\frac{ND}{\pi D}\right)\left\{1+3.2\left(\frac{\nu\Gamma D}{g_L\rho N d^4}\right)^{1/4}\right\}+1\times 10^{-3}\beta\left(\frac{g_c\sigma L}{\nu\Gamma}\right)^{3/2}\left(\frac{\nu\Gamma N^3}{g_L\rho D^3}\right)^{5/8}\right]^{1/3}$$

$$\times \left[1-\left(\frac{Nd}{\pi D}\right)\left\{1+3.2\left(\frac{\nu\Gamma D}{g_L\rho Nd^4}\right)^{1/4}\right\}\right] \quad (11)$$

Cylindrical fins

$$\frac{h}{h_o}=\left[1-\left(\frac{Nd}{\pi D}\right)\left\{1+4.8\left(\frac{\nu\Gamma D}{g_L\rho Nd^4}\right)^{1/4}\right\}+4.5\times 10^{-4}\beta\left(\frac{g_c\sigma L}{\nu\Gamma}\right)^{3/2}\left(\frac{\nu\Gamma N^3}{g_L\rho D^3}\right)^{5/8}\right]^{1/3}$$

$$\times\left[1-\left(\frac{Nd}{\pi D}\right)\left\{1+4.8\left(\frac{\nu\Gamma D}{g_L\rho Nd^4}\right)^{1/4}\right\}\right] \quad (12)$$

All unknown coefficients have been lumped into the one constant, β, in Equations (11) and (12) which must be determined empirically.

The sum of the first two terms in the brackets on the right of Equations (11) and (12) is always less than or equal to one and makes little contribution to the variation of h/h_o for large values of h/h_o. By differentiating Equations (11) and (12) and setting the derivative equal to zero to find the value of $Nd/\pi D$ for maximum h/h_o gives

Rectangular Fins

$$\left(\frac{Nd}{\pi D}\right)_{opt}\approx\frac{5}{13}\left[\frac{1}{1+2.7\left(\frac{\nu\Gamma D}{g_L\rho Nd^4}\right)^{1/4}}\right] \quad (13)$$

Cylindrical Fins

$$\left(\frac{Nd}{\pi D}\right)_{opt}\approx\frac{5}{13}\left[\frac{1}{1+4.0\left(\frac{\nu\Gamma D}{g_L\rho Nd^4}\right)^{1/4}}\right] \quad (14)$$

substantially independent of the value of the empirical constant, β.

EXPERIMENTAL EQUIPMENT AND PROCEDURE

The test section consisted of two vertical concentric tubes, a 1 in. I.D. × 43 in. long glass pipe with removable insulation to permit visual inspection of the mode of condensation, and a ½ in. O.D. × 4 ft. long aluminum condenser tube with a 0.028 in. thick wall. The overall cooled length of the condenser tube was 42½ in. The upper end of the condenser tube was connected to a steam chest maintained at a pressure of 4 to 5 lb./sq. in. guage. The steam pressure was used to determine the steam temperature. Inlet and outlet fluid temperatures were measured with iron-constantan thermocouples inserted in baffled mixing chambers at the entrance and exit of the test section. Liquid flow rates were determined with a calibrated rotameter and condensation rates were measured by collecting condensate. The pressure gradient along the annulus was measured between the steam chest and the sight glass at the exit of the condenser tube.

Finned Tubes

The rectangular finned tubes were manufactured by clamping the fins to the tubes at intervals. Because the fins had little rigidity, it was assumed that there was poor thermal contact between the fin and the tube wall over the bulk of the fin length. The clamps were U-shaped and were pinched against the fins every 4 in. along the fin. A ring was spot welded to the clamps around the outside of the fins to maintain their relative positions. The clamps fitted over the outside edge of the fins in order not to interrupt the flow of the thin film down the tubes. The primary reason that the fins were clamped to the tube (rather than being an integral part of the tube) was to permit study of the hydrodynamic effects of rivulet formation as free as possible from any conduction effects through the fins. The fins were made from aluminum; dimensions were 1/16 × 1/16 in., 1/8 × 0.013 in., 1/16 × 0.008 in.; the length was 40 in.

Procedure and Calibration

While the system was heating up, steam was vented to the atmosphere to remove noncondensables. When the system reached operation temperature, the vent was closed. Steady state was assumed to exist after the inlet and exit water temperatures and the condensate level in the sight glass had remained steady for at least one-half hour. Visual inspection of the tube surface indicated that dropwise condensation did not occur during any of the tests.

EXPERIMENTAL RESULTS

Measurements of the overall heat transfer coefficient as a function of cooling water velocity were made for four different ranges of mean temperature differences, Δt, between the condensing steam and the water coolant both with and without fins; typical values of Δt were 7 to 8°F., 11 to 13°F., 47 to 60°F., and 104 to 112°F.; the heat flux range was 2×10^4 to 10^5 B.t.u./hr. sq. ft. Wilson plots (that is, plots of the reciprocal of the heat transfer coefficient vs. the reciprocal of the cooling water velocity to the eight-tenths power) were prepared for constant heat fluxes from plots of heat transfer coefficient vs. heat flux. Assuming that the heat transfer resistances are additive, the intercept on the Wilson plot is the resistance of the metal wall plus the condensate film (*10*). Since the resistance of the metal wall is known, the condensing heat transfer coefficient can be easily calculated. In all cases the heat transfer coefficient was based on the area of the tube alone (that is, the area of the fin was not included in the tube area for the heat transfer coefficient calculation).

Heat balances, expressed as the ratio of total rate of heat transfer from condensate, q_{cond}, to total rate of heat transfer from axial temperature rise, $q_{\Delta T}$, were within ±5% for over 98% of the tests; the ratio $q_{cond}/q_{\Delta T}$ was 1.00 with a standard deviation of 0.028. Forced convection heat transfer coefficients in the absence of turbulence promoters were within ±12% of the Sieder-Tate relation (*11*)

$$\frac{h}{c_pG}=0.027\,N_{Re}^{-0.2}N_{Pr}^{-2/3}(\mu/\mu_w)^{0.14} \quad (15)$$

evaluated by the Wilson plot technique (*10*). Condensing heat transfer coefficients for the aluminum tube in the absence of wires (Figure 2) were in excellent agreement with Rohsenow, Webber, and Ling's (*12*) and with Dukler's (*13*) correlation for film condensation on a vertical surface with appreciable vapor shear. The interfacial shear was calculated directly from measured pressure drop data by using Lehtinen's (*15*) recommendation for calculating

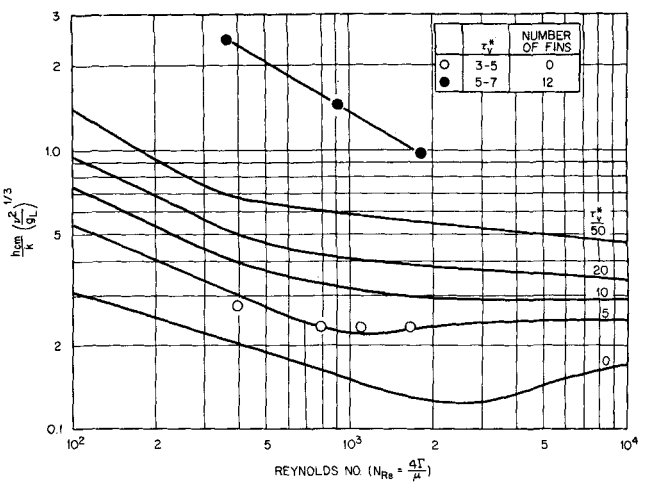

Fig. 2. Comparison of finned and plain tube condensing coefficients with Rohsenow's theory for film condensation on a vertical tube.

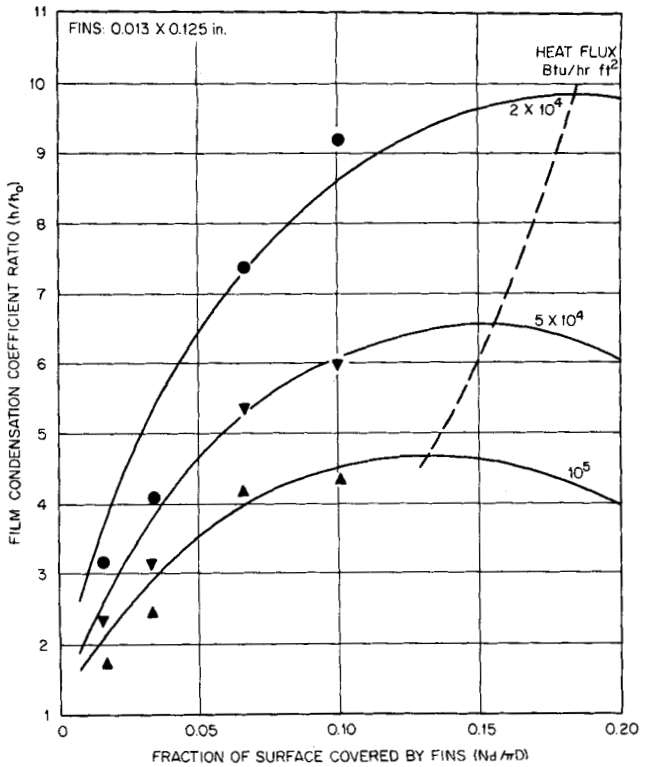

Fig. 3. Effect of rectangular fins on the enhancement of the film condensation heat transfer coefficient [solid lines calculated from model, Eq. (11); dashed line is calculated optimum from Eq. (13)].

the average mass velocity of the vapor, and was in good agreement with Bergelin's (*14*) correlation for the friction factor for gas flowing in a tube with a liquid layer on the wall.

Rectangular Fins

The maximum increase in film condensing coefficient was observed with twelve fins. The results are shown in Figure 2 which also contains the smooth tube calibration data. The marked increase caused by the fins is evident.

The relative enhancement of film condensation coefficients caused by small rectangular fins is illustrated in Figure 3, in which h/h_o (the ratio of experimentally determined heat transfer coefficients with and without fins) is plotted as a function of the fraction of the surface covered by fins, $Nd/\pi D$, with the heat flux as a parameter. The solid curves shown on Figure 3 were calculated from Equation (11) using a value for β of 8.20×10^{-3}. The dashed curve gives the value $(Nd/\pi D)_{opt}$ calculated from Equation (13).

Figure 3 shows that the enhancement increases rapidly with number of rectangular fins until about 10% of the surface is covered by fins. The simplified model agrees well with the data up to this fraction of surface coverage and then predicts a rather broad maximum over which addition of more fins causes little additional increase in condensing coefficient. Figure 3 also shows that the effect of the fins is greater when the heat flux is smaller. The maximum film condensation heat transfer coefficient observed with rectangular fins was 15,000 B.t.u./hr. sq. ft. °F. at a heat flux of 2×10^4 B.t.u./hr. sq. ft. using twelve $\frac{1}{8} \times 0.013$ in. fins. For these same conditions the condensing heat transfer coefficient of the tube without fins was 1,620 B.t.u./hr. sq. ft. °F. (The fins had substantially the same surface area as the tube, thus the total surface of the finned tube was about twice that of the plain tube.) The maximum uncertainty occurred at the greatest enhancement and was ±15%.

Flooding

Flooding will occur when the amount of condensate is sufficiently great so that the capacity of the fin to carry off the condensate as a rivulet is exceeded; that is, flooding will occur when the radius of curvature of the rivulet is greater than the rectangular fin height (or greater than the radius of cylindrical fins). The radius of curvature of the rivulet may be calculated from Equation (10). However, calculations indicated that rectangular fin heights less than 1/32 in. would be required to observe flooding for tube dimensions and heat fluxes used in the present study. Because of fabrication difficulties with rectangular fins, additional tests were made with cylindrical fins similar to those used in the previous study (*7*). Figure 4 summarizes all of the data for rectangular and cylindrical fins plotted as $[(h_{exp}/h_{calc}) - 1]$ vs. R/H or $R/(d/2)$. The data scatter around $[(h_{exp}/h_{calc}) - 1] = 0$ for values of R/H or $R/(d/2) < 1$ but are consistently below zero for all values of $R/(d/2) > 1$. Thus Figure 4 demonstrates the internal consistency of the model and suggests that flooding will occur where

Rectangular Fins

$$\frac{R}{H} = 3.2 \left(\frac{\nu \Gamma D}{g_L \rho N H^4} \right)^{1/4} > 1 \qquad (16)$$

Cylindrical Fins

$$\frac{R}{(d/2)} = 4.77 \left(\frac{\nu \Gamma D}{g_L \rho N d^4} \right)^{1/4} > 1 \qquad (17)$$

Fin Shape Comparison

The effect of fin size and shape on the enhancement of the film condensation coefficient by four fins is illustrated in Table 2 for a variety of fins at three different heat

Table 2. Effect of Fin Size and Shape on the Enhancement of the Film Condensation Coefficient by Four Fins

Series	Shape	Dimensions cross-section	Dimensions length	A_f/A	h/h_o heat Flux, 10^{+4} B.t.u./hr. sq. ft. 10	5	2
1*	C†	0.032 diam.	40	1.24	1.57	2.03	3.14
2	C	0.062 diam.	40	1.50	1.92	2.68	3.28
3	R‡	1/16 × 0.008	40	1.32	2.83	4.00	4.50
4	R	1/8 × 0.013	40	1.64	2.45	3.12	4.07
5	R	1/16 × 1/16	20§	1.16	1.49	1.92	1.96
6	R	1/16 × 1/16	20¶	1.16	1.67	2.56	3.50
7	R#	1/16 × 1/16	40	1.32	3.53	4.20	4.90

* Data from (*7*).
† C = cylindrical.
‡ R = rectangular.
§ Top half of tube.
¶ Bottom half of tube.
# Fins brazed to tube.

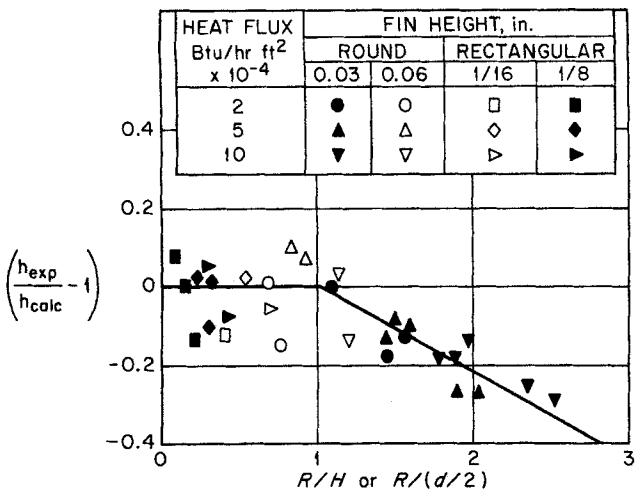

Fig. 4. Effect of fin height on reduction of film condensation coefficient due to flooding of tube surface.

flures. All of the full length rectangular fins gave greater enhancement than the full length cylindrical fins (7) when compared at the same heat flux (series 1 and 2 vs. series 3, 4, and 7). The enhancement caused by 1/16 in. high rectangular fins was substantially the same as that caused by ⅛ in. high rectangular fins despite the fact that the ratio (tube plus fin area)/(tube area) was 0.32 and 0.64, respectively (series 3 vs. series 4). As would be expected, four half-length fins on the bottom half of the tube gave greater enhancement than four half-length fins on the top half of the tube (series 5 vs. series 6). Finally it is not clear whether the greatest enhancement was observed with the series 7 rectangular fins because of their good thermal contact with the tube or whether the good mechanical contact with the tube caused less hindrance to rivulet formation.

Fluted Tubes

Data for the enhancement of film condensation by fluted tubes (*1* to *4*, *16*) and cylindrical fins (*7*) are compared in Figure 5 with the maximum enhancement values for rectangular fins found in the present study. Data for

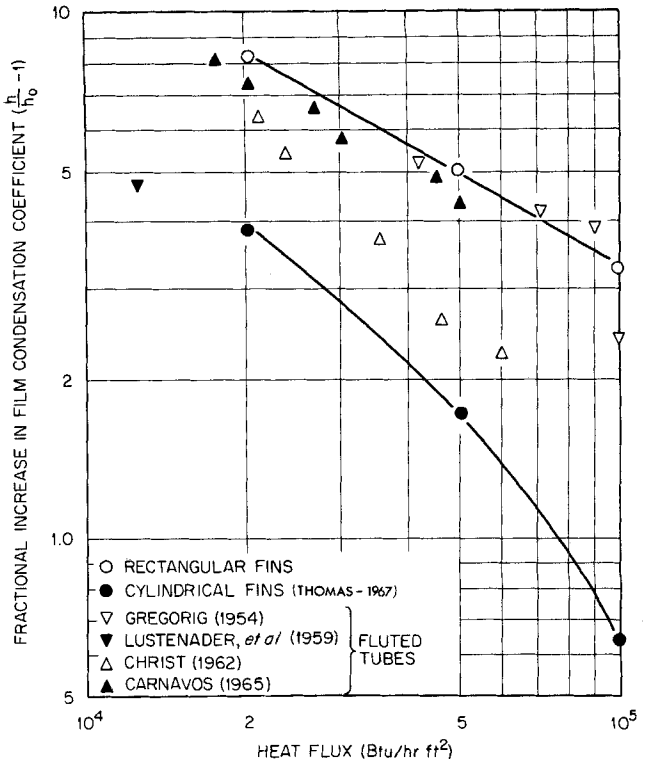

Fig. 5. Comparison of the effect of fluted and finned tubes on the film condensation heat transfer coefficient.

the present study were twice as long as the fluted tubes having the greatest effect on the condensing coefficient. It is of interest to note that the number of fins or flutes per inch of tube circumference (last column of Table 3) for the high performance surfaces are the same order of magnitude. Furthermore, by using the values of fraction of fluted tube surface over which the heat flow is concentrated as quoted in the fluted tube papers, (*1*, *16*) the numerical constant, β, for fluted tubes calculated from a simplified model analogous to Equation (4) of the present paper, was substantially the same as that found for the rectangular and cylindrical fin geometries.

Table 3. Comparison of Optimum Finned and Fluted Tube Geometries

	Tube length, ft.	O.D., in.	Crest to trough, in.	Total no. of fins or flutes, N	No. of fins or flutes per in. of circumference $\frac{N}{\pi D}\frac{1}{\text{in.}}$
Rectangular Fins	3.54	0.50	0.125	12	7.6
Cylindrical Fins*	3.54	0.50	0.030	12	7.6
Gregorig (1954)	1.72	0.75	0.023	29	12.2
Lustenader (1959)	2	3	0.034	(162)	17.2
Christ (1962)	13.1	†	†	(22)	†
Carnavos (1965)	1	3⅜	(0.049)	80	7.5

* Thomas (1967).
† Not available.
(Values in parentheses are estimated from drawings or photographs).

various tube geometries are given in Table 3 and the shapes are illustrated in Figure 1. The heat transfer coefficient data from the present study and from the study of Lustenader (*2*), and Carnavos (*3*) are based on the nominal tube diameter; insufficient data were given in the other papers (*1*, *16*) to determine the basis for their heat transfer coefficient calculations.

Figure 5 shows that at any given heat flux the present data for rectangular fins compare favorably with the fluted tube data despite the fact that the tubes used in

CONCLUSIONS

Vertical rectangular fins loosely attached to a vertical tube were found to increase the film condensation heat transfer coefficient by greater than a factor of nine at a heat flux of 2×10^4 B.t.u./hr. sq. ft. Fins with rectangular cross section gave markedly greater increases in performance than fins with circular cross section (7). Two factors which are believed to be important in causing this

difference are the smaller resistance to rivulet flow in the corner of the rectangular fin to tube junction (as compared with resistance to rivulet flow at the cylindrical fin to tube junction), and the smaller fraction of tube surface blocked by the rectangular fins as compared with cylindrical fins, thus making more tube surface available for the high transfer, thin film mode of condensation. The fact that the curvature radius of the rivulet of waters free surface is determined by the requirement that the sum of the internal and surface free energy be a minimum (5), and the fact that the constant value for the empirical coefficient β in Equations (11) and (12) (see Table 1) for two different fin shapes, support the belief that the shape of the fin is not an important factor in developing the surface tension force responsible for drawing the bulk of the condensate to the vicinity of the fin where it flows rapidly down the tube.

Loosely attached (clamped) fins were chosen for this study to permit evaluation of the effect of rivulet formation with as little interference as possible from conduction through the fins. However, the data for brazed fins in Table 2 indicate that integral fins may produce a greater increase of the heat transfer coefficient than loosely attached fins. Additional studies are required to determine the magnitude of the conduction effect.

Rectangular fins increased the average film condensation coefficients to values comparable to those observed with fluted tubes. Rectangular fins possess two distinct advantages over fluted tubes which are formed by fluting the surface of a thick walled tube or by fluting both the interior and exterior surface:

1. The thin film, high heat transfer mode of condensation occurs on the finned tube surface in the region between the rectangular fins. Thus, the thickness of the metal tube (and hence the resistance to heat transfer) can be minimized consistent with the requirements of tube strength and corrosion allowance. In contrast, the thin film, high heat transfer mode occurs on the crest of the flute beneath which the thickness of metal is often a maximum.

2. Finned tubes can be manufactured with a smooth inner surface of any other desired shape to take advantage of the optimum turbulence promotor configuration on that side of the tube for any given application.

ACKNOWLEDGMENT

The author wishes to acknowledge the support and suggestions of Kurt A. Kraus and the assistance of P. H. Hayes in performing the experimental measurements.

This research was jointly sponsored by the Office of Saline Water, U.S. Department of The Interior and the U.S. Atomic Energy Commission under contract with the Union Carbide Corporation.

NOTATION

A = surface area of tube, sq. ft.
A_f = surface area of tube plus fins, sq. ft.
A_1 = rivulet cross section area, sq. ft.
B = cross-sectional area of film between wires, sq. ft.
c_p = specific heat, B.t.u./lb.$_m$
d = wire diameter or fin width, ft.
D = tube diameter, ft.
D_H = hydraulic diameter for rivulet, ft.
f = Fanning friction factor, Equation (6), dimensionless
G = mass flow rate, lb.$_m$/sq. ft. hr.
g_c = conversion factor, (lb.$_m$/lb.$_f$) (ft./sq. hr.)
g_L = gravitational acceleration, ft./sq. hr.
H = height of fin, ft.
h = heat transfer coefficient with fins, B.t.u./(hr.) (sq. ft.) (°F.)
h_o = heat transfer coefficient without fins, B.t.u./(hr.) (sq. ft.) (°F.)
L = tube length, ft.
l = width of thin film between wires, ft.
N = number of wires or fins, dimensionless
N_{Re} = Reynolds number, dimensionless
N_{Pr} = Prandtl number, dimensionless
p = pressure, lb.$_f$/sq. ft.
P = wetted perimeter for rivulet, ft.
q/A = heat flux, B.t.u./(hr.) (sq. ft.)
R = radius of curvature, ft.
V = velocity, ft./sec.

Greek Letters

α = constant in Equation (2) = 1.72×10^{-6}, dimensionless
α_1 = constant in Equation (4), dimensionless
α_3 = constant in Equation (6), dimensionless
α_4 = constant in Equation (10), dimensionless
β = constant in Equations (11) and (12) = 8.2×10^{-3}, dimensionless
Γ = mass flow per unit perimeter, lb.$_m$/(hr.) (ft.)
μ = viscosity, lb.$_m$/(ft.) (sec.)
ν = kinematic viscosity, sq. ft./hr.
π = 3.1415 . . .
ρ = density, lb.$_m$ cu. ft.
σ = surface tension, lb.$_f$/ft.
τ_w = wall shear stress, lb.$_f$/sq. ft.

Subscripts

A = area A_1
B = area B
calc. = calculated from Equation (11) or (12)
exp = experimental value
f = fluid
opt = optimum
w = wall

LITERATURE CITED

1. Gregorig, Romano, *Z. Angew. Math. Phys.*, **5**, 36 (1954).
2. Lustenader, E. L., R. Richter, and F. J. Neugebauer, *J. Heat Transfer*, **81**, 297 (1959).
3. Carnovas, T. C., paper presented at the 1st Int. Symp. Water Desalination, Washington, D. C. (October 1965) Paper SWD/17.
4. Richter, R., ME thesis, Rensselaer Polytechnic Inst. (June 1958).
5. Landau, L. D., and Lifshitz, "Fluid Mechanics," Pergamon Press, New York (1959) p. 230.
6. Nusselt, W., *Z. VID*, **60**, 541, 569 (1916).
7. Thomas, D. G., *Ind. Eng. Chem., Fundamentals*, **6**, 97 (1967).
8. Fulford, G. D., Ph.D. thesis, Univer. Birmingham, Alabama (1962).
9. Gunn, D. J., and C. W. Darling, *Trans. Inst. of Chem. Eng.*, **41**, 163 (1963).
10. Perry, J. H., editor, "Chemical Engineers Handbook," 3rd ed., McGraw-Hill, New York (1950) pp. 464-470.
11. Sieder, E. N., and C. E. Tate, *Ind. Eng. Chem.*, **28**, 1429 (1936).
12. Rohsenow, W. M., J. H. Webber, and A. T. Ling, *Trans. Am. Soc. Mech. Engrs.*, **78**, 1637 (1956).
13. Dukler, A. E., *Chem. Eng. Progr. Symp. Ser. No. 56*, **30**, 1 (1960).
14. Bergelin, O. P., et al., *Am. Soc. Mech. Engrs.*, Paper No. (1949) p. 19.
15. Lehtinen, J. A., Sc.D. thesis, Mass. Inst. Tech., Cambridge (June 1957).
16. Christ, A., *Escher Wyss News*, **35**, 94 (1962).

Manuscript received August 16, 1966; revision received September 14, 1967; paper accepted October 9, 1967.